

Article

Bioactive Phenolic Compounds from *Peperomia obtusifolia*

Ismail Ware ^{1,2} , Katrin Franke ^{1,*} , Hidayat Hussain ¹ , Ibrahim Morgan ¹ , Robert Rennert ¹ and Ludger A. Wessjohann ^{1,*} 

¹ Department of Bioorganic Chemistry, Leibniz Institute of Plant Biochemistry, D-06120 Halle, Germany; ismailbin.ware@ipb-halle.de (I.W.); hidayat.hussain@ipb-halle.de (H.H.); ibrahim.morgan@ipb-halle.de (I.M.); robert.rennert@ipb-halle.de (R.R.)

² Institute of Bioproduct Development, Universiti Teknologi Malaysia, Johor Bahru 81310, Malaysia

* Correspondence: katrin.franke@ipb-halle.de (K.F.); ludger.wessjohann@ipb-halle.de (L.A.W.); Tel.: +49-345-5582-1380 (K.F.); +49-345-5582-1300 (L.A.W.)

Abstract: *Peperomia obtusifolia* (L.) A. Dietr., native to Middle America, is an ornamental plant also traditionally used for its mild antimicrobial properties. Chemical investigation on the leaves of *P. obtusifolia* resulted in the isolation of two previously undescribed compounds, named peperomic ester (**1**) and peperoside (**2**), together with five known compounds, viz. *N*-[2-(3,4-dihydroxyphenyl)ethyl]-3,4-dihydroxybenzamide (**3**), becatamide (**4**), peperobtusin A (**5**), peperomin B (**6**), and arabinothalictoside (**7**). The structures of these compounds were elucidated by 1D and 2D NMR techniques and HREIMS analyses. Compounds 1–7 were evaluated for their anthelmintic (against *Caenorhabditis elegans*), antifungal (against *Botrytis cinerea*, *Septoria tritici* and *Phytophthora infestans*), antibacterial (against *Bacillus subtilis* and *Aliivibrio fischeri*), and antiproliferative (against PC-3 and HT-29 human cancer cell lines) activities. The known peperobtusin A (**5**) was the most active compound against the PC-3 cancer cell line with IC₅₀ values of 25.6 μM and 36.0 μM in MTT and CV assays, respectively. This compound also induced 90% inhibition of bacterial growth of the Gram-positive *B. subtilis* at a concentration of 100 μM. In addition, compound **3** showed anti-oomycotic activity against *P. infestans* with an inhibition value of 56% by using a concentration of 125 μM. However, no anthelmintic activity was observed.

Keywords: Piperaceae; *Peperomia obtusifolia*; isolation; cytotoxicity; anticancer; antibacterial



Citation: Ware, I.; Franke, K.; Hussain, H.; Morgan, I.; Rennert, R.; Wessjohann, L.A. Bioactive Phenolic Compounds from *Peperomia obtusifolia*. *Molecules* **2022**, *27*, 4363. <https://doi.org/10.3390/molecules27144363>

Academic Editor: Jacqueline Aparecida Takahashi

Received: 8 June 2022

Accepted: 5 July 2022

Published: 7 July 2022

Publisher's Note: MDPI stays neutral with regard to jurisdictional claims in published maps and institutional affiliations.



Copyright: © 2022 by the authors. Licensee MDPI, Basel, Switzerland. This article is an open access article distributed under the terms and conditions of the Creative Commons Attribution (CC BY) license (<https://creativecommons.org/licenses/by/4.0/>).

1. Introduction

Peperomia is one of the two major genera of the Piperaceae family, with approximately 1700 species common in almost all tropical areas [1]. Plants of the genus *Peperomia* possess numerous uses as traditional medicine to treat asthma, gastric ulcers, bacterial infection, pain, and inflammation [2]. *Peperomia* species produce several classes of secondary metabolites such as flavonoids, secolignans, prenylated phenolic substances, chromenes, polyketides [3], lignans, tetrahydrofurans, terpenoids, meroterpenoids, and amides [1,4,5]. Some compounds from *P. pellucida*, *P. doclouxii*, *P. dindygulensis*, and *P. blanda* were reported to exhibit cytotoxic effects [2,6–8].

Peperomia obtusifolia (L.) A. Dietr. is widely distributed from Mexico to the northern part of South America. It is widely known as *baby rubber* or the *paragua* plant. In spite of its dominating decorative use, some communities in Central America use this plant to treat insect and snake bites and also as a skin cleanser [9]. Previous studies on *P. obtusifolia* resulted in the isolation of chromanes, flavonoids, lignans, and other secondary metabolites [10–14]. Several biological activities were described for compounds isolated from this species, such as trypanocidal [11], anti-inflammatory [15], and antibacterial activities [14]. In the present study, we report the isolation, structure elucidation, and biological effects of two previously undescribed compounds (**1** and **2**), along with five known compounds (**3**–**7**) from the methanolic leaf extract of *P. obtusifolia*.

2. Results and Discussion

The dried leaves of *P. obtusifolia* were extracted with 80% aqueous methanol. The crude extract was suspended in water and successively fractionated by liquid–liquid partition between water and *n*-hexane, and water and ethyl acetate. The constituents were purified by preparative HPLC and repeated column chromatography on silica gel, Sephadex LH20, and Diaion HP20, which yielded two previously undescribed compounds (**1** and **2**), as well as two amide derivatives (**3** and **4**), a chromane (**5**), a secolignan (**6**), and an unusual phenolic nitroalkyl diglycoside (**7**) (Figure 1). The chemical structures of **1** and **2** were elucidated by detailed spectroscopic techniques.

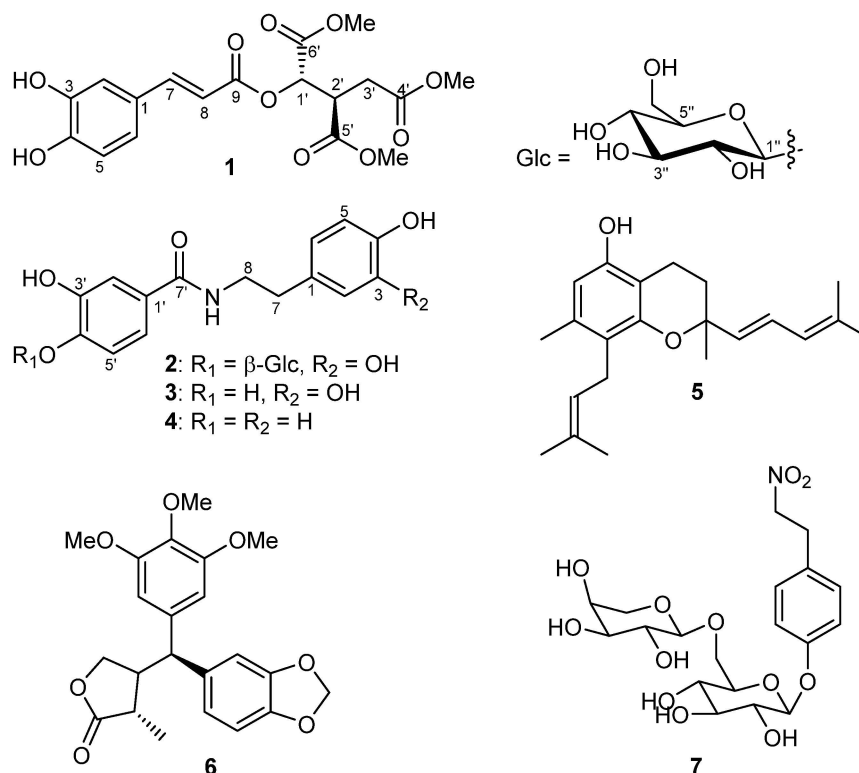


Figure 1. Chemical structures of compounds **1**–**7**.

Compound **1** was obtained as a brownish liquid from the aqueous fraction. The HR-ESI-MS measurements of the deprotonated molecular ion at m/z 395.0975 $[M - H]^-$ indicated the molecular formula $C_{18}H_{20}O_{10}$. The IR spectrum revealed the presence of hydroxyl (3402 cm^{-1}) and carbonyl groups (1715 cm^{-1}). Inspection of the ^1H NMR data (Table 1) exhibited characteristic signals of an ABX aromatic system at δ 7.06 (1H, d, $J = 2.1\text{ Hz}$, H-2), 6.79 (1H, d, $J = 8.2\text{ Hz}$, H-5), and 6.97 (1H, d, $J = 8.2, 2.1\text{ Hz}$, H-6) and of one *E*-configured double bond [δ 7.59 (1H, d, $J = 15.8\text{ Hz}$, H-7) at 6.29 (1H, d, $J = 15.8\text{ Hz}$, H-8)]. In addition, ^1H NMR data also showed the presence of two saturated methine groups [δ 5.46 (1H, d, $J = 3.9\text{ Hz}$, H-1') at 3.62 (1H, ddd, $J = 9.0, 5.5, 3.9\text{ Hz}$, H-2'), and one methylene group [δ 2.85 (1H, dd, $J = 17.2, 9.0\text{ Hz}$, H-3'a) at 2.66 (1H, d, $J = 17.2, 5.5\text{ Hz}$, H-3'b)] along with three methoxy groups at δ 3.68, 3.73, and 3.77. The ^{13}C data (Table 1) exhibited one sp^2 quaternary carbon [δ_{C} 127.4 (C-1)], two oxygenated sp^2 tertiary carbons [δ_{C} 146.8 (C-3), 150.0 (C-4)], and four carbonyl groups [δ_{C} 167.5 (C-9), 173.2 (C-4'), 170.2 (C-5'), 172.1 (C-6')]. The scaffold of compound **1** was established by an HMBC experiment, showing long-range correlations from H-7 to C-1, C-2, C-6, C-8, and C-9, indicating that the aromatic ring and the carbonyl group C-9 were linked to C-7 in the form of a caffeic acid moiety. In addition, COSY correlations of H-1'/H-2', H-2'/H-1'/H-3'a/H-3'b, H-3'a/H-2', and H-3b/H-2', together with HMBC correlations of the three methoxy groups to their respective carbonyls (C-4', C-5', and C-6') and HMBC correlations of H-1' and C-2', C-3', C-5', C-6' and of H-2' and C-1',

C-3', C-4', C-5', and C-6' suggested the presence of an isocitrate core. The C-1' hydroxyl of the isocitrate unit is attached to the caffeic acid moiety at C-9 indicated by the long-range correlation from H-1' (δ_{H} 5.46) to C-9 (δ_{C} 167.5) (Figure 2). The methylated isocitrate moiety of **1** is similar to those found in cryptoporin acids isolated from *Cryptoporus sinensis* [16] and *Cryptoporus volvatus* [17,18], which are also conjugates of isocitrate. Since compound **1** was also detected in an ethanolic crude extract (Figure S9), the methylation is not a processing artifact. The absolute configuration of C-1' and C-2' of the isocitrate group was suggested to be (1'S,2'R) by comparison of its optical rotation sign (negative optical rotation value) with published compounds having a (1'R,2'S) absolute configuration and opposite-in-sign specific rotation (positive optical rotation value) [16,19]. Thus, the methylated isocitrate moiety is in accordance with an L-threo-isocitric acid core ((1S,2R)-1-hydroxypropane-1,2,3-tricarboxylic acid). Based on the above-mentioned evidence, the structure of **1** was elucidated as trimethyl (1S,2R)-1-(((E)-3-(3,4-dihydroxyphenyl)acryloyl)oxy)propane-1,2,3-tricarboxylate and given the trivial name peperomic ester.

Table 1. ^1H - and ^{13}C -NMR data of **1** (in CD_3OD ; δ in ppm, J in Hz).

No.	δ (H) ^a	δ (C) ^b	HMBC
1	-	127.4	
2	7.06 (d, $J = 2.1$)	115.2	
3	-	146.8	
4	-	150.0	
5	6.79 (d, $J = 8.2$)	116.5	
6	6.97 (dd, $J = 8.2, 2.1$)	123.3	
7	7.59 (d, $J = 15.8$)	148.6	C1, C2, C6, C8, C9
8	6.29 (d, $J = 15.8$)	113.4	C1, C7, C9
9	-	167.5	
1'	5.46 (d, $J = 3.9$)	72.6	C2', C3', C5', C6', C9'
2'	3.62 (ddd, $J = 9.0, 5.5, 3.9$)	44.2	C1', C3', C4', C5', C6'
3'a	2.85 (d, $J = 17.2, 9.0$)	32.8	C2', C1', C4', C6'
3'b	2.66 (d, $J = 17.2, 5.5$)	32.8	C2', C1', C4', C6'
4'	-	173.2	
5'	-	170.2	
6'	-	172.1	
OMe	3.73	52.9	C6'
OMe	3.77	53.1	C5'
OMe	3.68	53.4	C4'

^a Recorded at 400 MHz. ^b Recorded at 100 MHz.

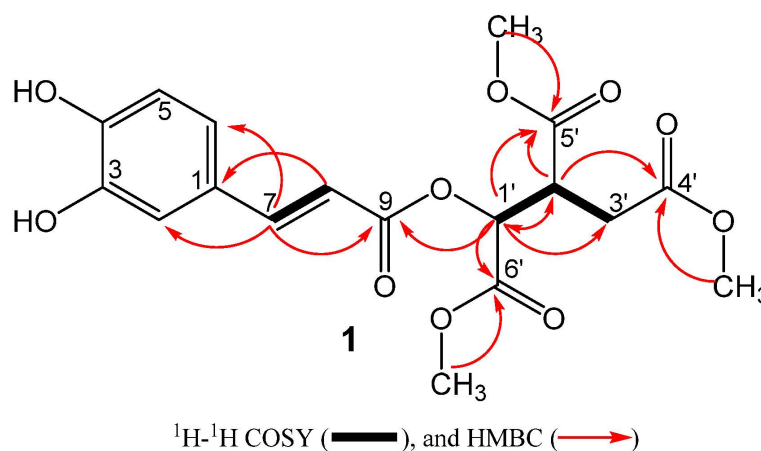


Figure 2. Key ^1H - ^1H COSY and HMBC correlation of **1**.

Compound **2** (Figure 3) was obtained as a white amorphous powder from the ethyl acetate fraction. The HR-ESI-MS measurements of the deprotonated molecular ion at m/z 450.1379 $[\text{M} - \text{H}]^-$ indicated the molecular formula $\text{C}_{21}\text{H}_{25}\text{NO}_{10}$. The IR spectrum

displayed absorption for hydroxyl (3250 cm^{-1}) and carbonyl groups (1607 cm^{-1}). The NMR data of compound **2** (Table 2, Figure 3) show the presence of an *N*-[2-(3,4-dihydroxyphenyl)ethyl]-3,4-dihydroxybenzamide moiety [20]. The structure of the aglycon part is the same as in compound **3**.

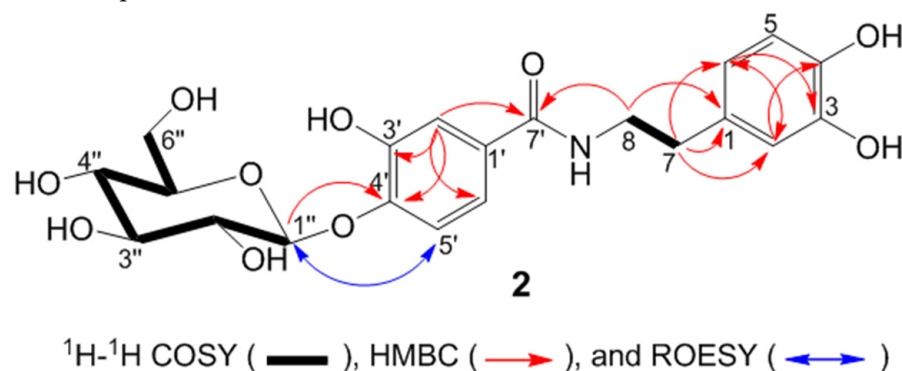


Figure 3. Key ^1H - ^1H COSY, HMBC, and ROESY correlation of **2**.

Table 2. ^1H - and ^{13}C -NMR data of **2** (in CD_3OD ; δ in ppm, J in Hz).

No.	δ (H) ^a	δ (C) ^b	HMBC
1	-	132.2	
2	6.70 (d, $J = 2.1$)	117.0	C1, C3, C4, C6, C7
3	-	144.7	
4	-	146.2	
5	6.69 (d, $J = 8.0$)	116.5	C1, C3, C4, C6, C7
6	6.59 (dd, $J = 8.0, 2.1$)	121.1	C2, C3, C7
7	2.75 (t, $J = 7.6$)	35.9	C1, C2, C6, C8
8a	3.57 (dt, $J = 13.2, 7.6$)	42.8	C1, C7, C7'
8b	3.50 (dt, $J = 13.2, 7.6$)	42.8	C1, C7, C7'
1'	-	126.3	
2'	7.25 (d, $J = 3.1$)	120.7	C1', C3', C4', C5', C6', C7'
3'	-	154.3	
4'	-	150.1	
5'	7.24 (d, $J = 8.8$)	117.3	C1', C3', C4', C6'
6'	6.86 (dd, $J = 8.8, 3.1$)	120.3	C1', C3', C4', C5'
7'	-	167.8	
1''	4.79 (d, $J = 7.5$)	105.1	C4', C3'', C5''
2''	3.38 (m)	74.9	
3''	3.41 (m)	78.1	
4''	3.38 (m)	78.5	
5''	3.39 (m)	71.3	
6a''	3.70 (dd, $J = 12.0, 5.0$)	62.5	
6b''	3.89 (d, $J = 12.0$)	62.5	

^a Recorded at 400 MHz. ^b Recorded at 100 MHz.

In addition, NMR data indicate the presence of an anomeric carbon [$(\delta_{\text{H}} 4.79$ (1H, d, $J = 7.5$ Hz); $\delta_{\text{C}} 105.1$] together with four methine carbon signals between 71.3 and 78.5 ppm, which is typical for glucose. The coupling constant value of the sugar anomeric proton ($J = 7.5$ Hz) revealed the β -configuration of the glucosyl moiety. The linkage of C-1'' from the sugar moiety to 4'OH of the 3,4-dihydroxybenzoate moiety was established based on the HMBC long-range correlation from H-1'' ($\delta_{\text{H}} 4.79$) to C-4' ($\delta_{\text{C}} 150.1$) (Figure 3). This conclusion is supported by the ROESY correlation of H-1'' ($\delta_{\text{H}} 4.79$) with H-5' ($\delta_{\text{H}} 7.24$). From the above spectroscopic data, the structure of compound **2** was established as *N*-[2-(3,4-dihydroxyphenyl)ethyl]-3,4-dihydroxybenzamide 4'-*O*- β -D-glucoside, given the trivial name peperoside.

The phytochemical investigation of the *P. obtusifolia* (L.) A.Dietr. leaves allowed the isolation of five other known compounds, *N*-[2-(3,4-dihydroxyphenyl)ethyl]-3,4-dihydroxybenzamide

(3) [20], becatamide (also known as houttuynamide A, 4) [21], peperobtusin A (5) [10], peperomin B (6) [22], and arabinothalictoside (7) [23]. These compounds were identified by comparing their MS and NMR spectral data with published data, which agree with the data reported for the respective compounds. Among the known constituents, compound 5 was already reported from *P. obtusifolia*, while compounds 3, 4, and 6 were isolated from other *Peperomia* species such as *P. duclouxii* [7], *P. tetraphylla* [24], and *P. japonica* [22], respectively. Compound 7 is an unusual nitro natural product which was isolated for the first time from the Japanese plant *Sagittaria trifolia* [25] and later reported in *Aristolochia fordiana* [26], which belong to Piperales and *Annona squamosa* [23].

Peperomia species constituents have previously been reported to exhibit a variety of biological activities, either as extracts or pure compounds [2,27–29]. Thus, the compounds isolated from this species were evaluated for their anthelmintic, antifungal, antibacterial, and anticancer properties. These biological examinations were conducted by using established non-pathogenic model organisms and human cancer cell lines (all BSL-1) in fast-screening assays (Tables 3 and 4).

Table 3. Anthelmintic (*Caenorhabditis elegans*), antifungal (*Botrytis cinerea*, *Septoria tritici* and *Phytophthora infestans*), and antibacterial (*Bacillus subtilis*, *Aliivibrio fischeri*) activities of isolated compounds (1–7) from *P. obtusifolia*.

Compound	Anthelmintic Assay		Antifungal Assays		Antibacterial Assays		
	Mortality [%]	Growth Inhibition [%] ^a				Growth Inhibition [%] ^a	
	<i>C. elegans</i>	<i>B. cinerea</i>	<i>S. tritici</i>	<i>P. infestans</i>	<i>B. subtilis</i>	<i>A. fischeri</i>	
1	200 µM	125 µM	125 µM	125 µM	100 µM ^b	100 µM ^b	
2	1.9 ± 0.8	−13.6 ± 17.3	−12.5 ± 17.9	10.1 ± 2.3	8.0 ± 19.0	−5.6 ± 2.60	
3	0.0 ± 0.0	−27.6 ± 7.6	21.8 ± 8.9	−51.5 ± 16.0	7.0 ± 15.0	−3.1 ± 1.80	
4	0.0 ± 0.0	−18.5 ± 3.1	−40.0 ± 35.2	56.2 ± 10.3	7.0 ± 2.8	−211.6 ± 27.6	
5	2.9 ± 1.4	−32.3 ± 28.7	−9.8 ± 8.3	−66.4 ± 30.4	−21.0 ± 28.0	−35.9 ± 19.4	
6	4.8 ± 1.4	27.0 ± 25.8	46.9 ± 8.3	−6.0 ± 64.4	90.0 ± 2.0	−32.7 ± 12.7	
7	2.0 ± 1.7	51.4 ± 22.3	−12.9 ± 2.3	−9.4 ± 27.4	−5.0 ± 51.0	30.4 ± 8.4	
7	1.7 ± 2.4	2.8 ± 19.5	−7.2 ± 1.9	17.1 ± 12.1	5.0 ± 17.0	1.6 ± 3.0	
Pos. control	10 µg/mL ivermectin	125 µM epoxiconazole	125 µM terbinafine	125 µM terbinafine	100 µM chloramphenicol	100 µM chloramphenicol	
	98.7 ± 1.9	92.0 ± 1.4	96.8 ± 1.2	96.8 ± 1.2	99.0 ± 0	100.0 ± 0	

^a Negative values indicate an increase in fungal or bacterial growth in comparison to the negative control (0% inhibition); ^b Growth inhibition rates below 50% indicate IC₅₀ values > 100 µM.

Table 4. Antiproliferative and cytotoxic activities of isolated compounds (1–7) from *P. obtusifolia* against human prostate (PC-3) and colorectal (HT-29) cancer cell lines.

Compound	Metabolic cell Viability (MTT)/Cytotoxicity (CV) Assays			
	Cell Viability/Survivals [%]			
	PC-3 (MTT Assay)	PC-3 (CV Assay)	HT-29 (MTT Assay)	HT-29 (CV Assay)
	10 µM	10 µM	10 µM	10 µM
1	101.4 ± 5.8	97.5 ± 4.1	100.3 ± 4.4	91.0 ± 5.1
2	84.1 ± 4.9	84.0 ± 6.9	74.9 ± 6.5	78.2 ± 4.4
3	90.6 ± 3.3	98.3 ± 1.3	82.6 ± 4.8	100.3 ± 3.7
4	114.4 ± 1.2	92.9 ± 5.0	111.9 ± 1.8	89.0 ± 3.0
5	2.4 ± 6.3	−3.4 ± 24.7	59.7 ± 20.5	82.5 ± 4.3
6	120.9 ± 4.3	93.7 ± 2.6	117.1 ± 3.0	88.2 ± 3.9
7	113.7 ± 4.0	112.2 ± 4.7	115.3 ± 3.9	107.5 ± 2.9

Digitonin (125 µM) was used as a positive control, compromising the cells to the point of 0% cell viability/cancer cell survival after 48 h.

The anthelmintic activity was evaluated against *Caenorhabditis elegans*, however, the compounds did not significantly kill the nematodes even when applying a high concentra-

tion of 200 μM . Moreover, most of the compounds tested for antifungal effects against the phytopathogens *B. cinerea*, *S. tritici*, and *P. infestans* were considered as inactive since the inhibition of fungal growth at a concentration of 125 μM was less than 50%. An exception was *N*-[2-(3,4-dihydroxyphenyl)ethyl]-3,4-dihydroxybenzamide (3), which displayed interesting anti-oomycotic activity against *P. infestans* with an inhibition value of 56% at the same concentration. For the antibacterial assays, the compounds were tested in concentrations of 1 and 100 μM . None of the compounds inhibited the Gram-negative bacterium *A. fischeri* even at the highest test concentration of 100 μM . However, against the Gram-positive *B. subtilis*, peperobtusin A (5) induced a 90% inhibition of bacterial growth when treating at a concentration of 100 μM , prompting further investigations against human pathogens. Prenylated benzopyrans seem to be the active principle of *Peperomia* against Gram-positive bacteria, including resistant *Staphylococcus aureus* and *Enterococcus faecalis* strains [14]. Since all other isolated compounds induced less than 50% inhibition of bacterial growth when applying a concentration of 100 μM (Table 3), their half-maximal inhibitory concentration (IC_{50}) values must be estimated to be greater than 100 μM .

Furthermore, the compounds 1–7 were screened for their potential antiproliferative or cytotoxic activity against two human cancer lines, namely prostate adenocarcinoma cells (PC-3) and colorectal adenocarcinoma cells (HT-29). The compounds' effect on the metabolic cancer cell viability was determined by conducting an MTT assay, general cytotoxic effects were determined by using a CV assay, both after 48 h cancer cell treatment with the compounds under investigation. A very potent permeabilizer of cell membranes, digitonin (125 μM), was used as a positive control, compromising the cells to the point of 0% of cell viability after 48 h. The compounds were tested at two different concentrations, namely 10 nM and 10 μM .

As shown in Table 4, most of the compounds exhibited no significant antiproliferative and cytotoxic effects on PC-3 and HT-29 cancer cells, with the exception of peperobtusin A (5), which strongly inhibited the viability and growth of PC-3 cells in an MTT and CV fast-screening assay after treating the cells with 10 μM of the compound for 48 h. Under the same fast-screening assay conditions, a moderate activity of compound 5 against the HT-29 colorectal cancer cell line was also observed.

Based on its antiproliferative and cytotoxic effects, as determined with a 10 μM concentration in the initial fast-screening assay, compound 5 was subjected to further evaluations of its IC_{50} values in both cancer cell lines. The cells were treated with increasing concentrations of up to 100 μM of compound 5 for 48 h, followed by an MTT and CV assay read-out, data analyses, and calculation of IC_{50} values. The IC_{50} values of compound 5 determined by MTT assay, indicating the metabolic viability of the cancer cells, were $25.6 \pm 2.8 \mu\text{M}$ and $45.5 \pm 8.8 \mu\text{M}$ in PC-3 and HT-29 cells, respectively (see Figure 4A). The CV assay, reflecting general cytotoxic and antiproliferative impacts, showed similar IC_{50} values of $36.0 \pm 4.1 \mu\text{M}$ and $58.1 \pm 11.2 \mu\text{M}$ for PC-3 and HT-29 cells, respectively (Figure 4B). However, given the result of the preliminary fast-screening (fixed concentration 10 μM) of compound 5, which estimated an IC_{50} value of less than 10 μM , the lower efficacy at the above actual calculated IC_{50} values based on the dose-response curves was unexpected, especially in the case of PC-3 cells. However, the IC_{50} values were reproduced in three different assay formats, each with 2-3 biological replicates, namely MTT, CV, and resazurin assays (data not shown), which revealed an IC_{50} range of 25–45 μM . This implies that fast-screening with a single concentration and a single biological replicate, although with technical quadruplicates, is only a very rough, initial estimation of the compounds' activity.

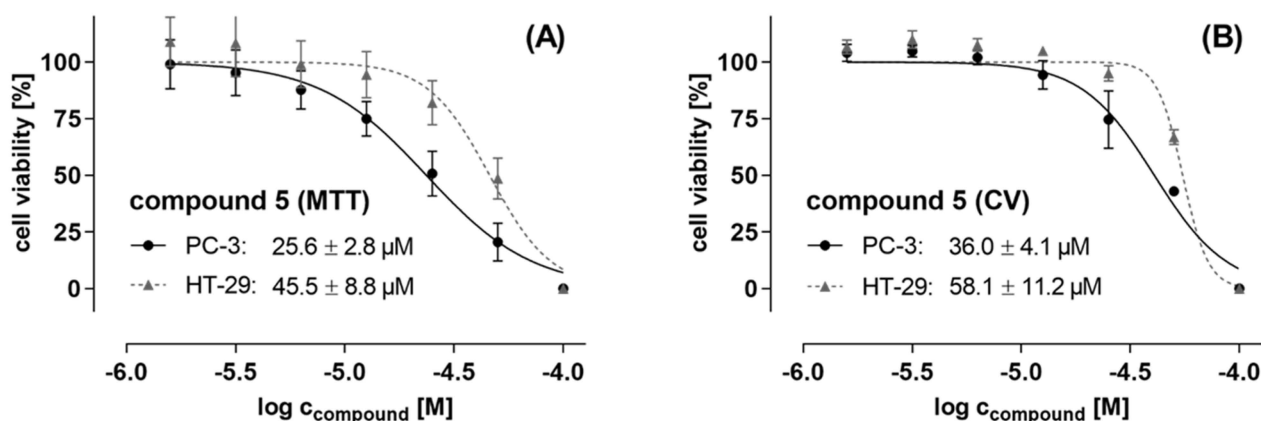


Figure 4. Effect of peperobtusin A (5) on (A) the metabolic cell viability of prostate PC-3 cancer cells and colon HT-29 cancer cells, as determined by MTT assay after 48 hours of cell treatment. (B) General cytotoxic and antiproliferative effect of 5 on both cancer cell lines under comparable treatment conditions, as determined by using crystal violet (CV) assay. Data represent biological duplicates, each comprising technical quadruplicates. IC₅₀ curves were analyzed and drawn using SigmaPlot and GraphPad Prism software, respectively. IC₅₀ values are given as mean ± SD.

Peperobtusin A (5) is a prenylated benzopyran with a chiral center at C-2. It was obtained with an optical activity of $[\alpha]_{\text{D}}^{20} 0$ (*c* 0.28, CHCl₃), implying a racemic mixture of the molecule. This result corroborated previously published data [11,30]. The compound was isolated before from the same species [10,11,14] and other *Peperomia* species, such as *P. tetraphylla* [31] and *P. clusiifolia* [32]. Although there are a few existing studies addressing the biological activities of peperobtusin A (5), this study is the first report related to the antiproliferative and cytotoxic effect against PC-3 (prostate) and HT-29 (colon) cancer cell lines. Previous investigations indicated the antitrypanosomal and antitumor potential of peperobtusin A. Regarding the antitrypanosomal activity, the compound with an IC₅₀ value of 3.1 μM was almost three times more active than the positive control benznidazole [11]. Furthermore, Da Silva Mota and collaborators also evaluated its cytotoxicity in mammalian cells (murine peritoneal macrophages) and found the compound to not be toxic at the concentration level of its trypanocidal activity [11]. A recent study by Shi et al [31] revealed that peperobtusin A (5) had antiproliferation effects against the human lymphoma cell line U937 with an IC₅₀ value of 63.26 μM at 24 h, however, exerted only minor effects on other human cancer cell lines such as human melanoma (A375), human bladder carcinoma (T24), and human breast epithelial cells (HBL-100). According to Shi et al. [31], the intracellular ROS formation and the activation of caspases and P38 MAPK played significant roles in the apoptosis induced by peperobtusin A. Therefore, in future investigations, the mode of action of peperobtusin A (5) in PC3 and HT29 cell lines should be addressed in detail and expanded; toxicological investigations should be performed to validate the safety of this compound before developing it as trypanocide.

3. Materials and Methods

3.1. General Methods

The following instruments were used to obtain physical and spectroscopic data: column chromatography was performed on silica gel (400–630 mesh, Merck, Darmstadt, Germany), Sephadex LH-20 (Fluka, Steinheim, Germany), and Diaion HP20 (Supelco, Bellefonte, PA, USA). Fractions and substances were monitored by TLC. TLC was conducted on precoated Kieselgel 60 F 254 plates (Merck, Darmstadt, Germany) and the spots were detected either by examining the plates under a UV lamp at 254 and 366 nm or by treating the plates with vanillin or natural product reagents. UV spectra were recorded on a Jasco V-770 UV-Vis/NIR spectrophotometer (Jasco, Pfungstadt, Germany), meanwhile specific rotation was measured with a Jasco P-2000 digital polarimeter (Jasco, Pfungstadt,

Germany). The IR (ATR) spectra were carried out in MeOH using a Thermo Nicolet 5700 FT-IR spectrometer (Thermo Nicolet Analytical Instruments, Madison, WI, USA).

NMR spectra were obtained with an Agilent DD2 400 system at +25 °C (Varian, Palo Alto, CA, USA) using a 5 mm inverse detection cryoprobe. The compounds were dissolved in CD₃OD (99.8% D) or CDCl₃ (99.8% D) and the spectra were recorded at 399.915 MHz (¹H) and 100.569 MHz (¹³C). One-dimensional (¹H and ¹³C) and two-dimensional (¹H,¹³C HSQC, ¹H,¹³C HMBC, ¹H,¹H COSY, and ¹H,¹H ROESY) spectra were measured using standard CHEMPACK 8.1 pulse sequences implemented in the Varian VNMRJ 4.2 spectrometer software (Varian, Palo Alto, CA, USA). ¹H chemical shifts are referenced to internal TMS (¹H δ = 0 ppm), while ¹³C chemical shifts are referenced to CD₃OD (¹³C δ = 49 ppm) or CDCl₃ (¹³C δ = 77.0 ppm).

The semi-preparative HPLC was performed on a Shimadzu prominence system (Kyoto, Japan) equipped with LabSolutions software, LC-20AT pump, SPD-M20A diode array detector, SIL-20A auto sampler, and FRC-10A fraction collector unit. Chromatographic separation was carried out using a YMC Pack C18 column (5 μm, 120 Å, 150 mm × 10 mm I.D, YMC, USA) using H₂O (A) and CH₃CN (B) as eluents at a flow rate of 2.2 mL min⁻¹.

The high-resolution mass spectra in both positive and negative ion modes were acquired using either an Orbitrap Elite Mass spectrometer or API 3200 Triple Quadrupole System. The Orbitrap Elite Mass spectrometer (ThermoFisher Scientific, Bremen, Germany) was equipped with an HESI electrospray ion source (spray voltage 4.0 kV, capillary temperature 275 °C, source heater temperature 80 °C, FTMS resolution 100,000), whereas the API 3200 Triple Quadrupole System (Sciex, Framingham, MA, USA) was equipped with a turbo ion spray source, which performs ionization with an ion spray voltage on 70 eV. During the measurement, the mass/charge range from 50 to 2000 was scanned.

3.2. Plant Material

The aerial part of *P. obtusifolia* (L.) A. Dietr. was collected in April 2018 at the Leibniz Institute of Plant Biochemistry (IPB), Halle (Saale), Germany from an ornamental plant grown for 20 years on an east oriented window sill. A voucher specimen (ISW010) was deposited in the IPB collection.

3.3. Extraction and Isolation

The fresh leaves (267.3 g) of *P. obtusifolia* were dried using a freeze drier and ground to powder form (29.7 g). The powdered material was extracted five times (1.0 L/each) with 80% aqueous methanol at room temperature, yielding 6.4 g of residue after evaporating the solvent in vacuo. The residue was suspended in H₂O (250 mL) and then successively partitioned with *n*-hexane and ethyl acetate, resulting in the two respective fractions (1.4 g *n*-hexane, 0.8 g EtOAc), as well as an aqueous fraction (3.6 g) (See Figure S20 for the isolation scheme).

Part of the EtOAc fraction (0.74 g) was chromatographed on a silica gel column and eluted with a stepwise gradient of CH₂Cl₂: MeOH (1:0 to 0:1) to give seven fractions (E1-E7). Fraction E1 (32.5 mg) underwent column chromatographic separation over a Sephadex LH-20 column (CH₂Cl₂/MeOH 1:1), affording four subfractions (A-D). Further separation of subfraction C (4.3 mg) over silica gel (CH₂Cl₂:MeOH 95:5–90:10) yielded becatamide (**4**, 1.4 mg, R_f = 0.25 in 5% MeOH in CH₂Cl₂) [21]. Fraction E2 (190.5 mg) was chromatographed over a Sephadex-LH20 column (100% MeOH) to afford an amorphous powder that was identified as *N*-[2-(3,4-dihydroxyphenyl)ethyl]-3,4-dihydroxybenz amide (**3**, 142.5 mg, R_f = 0.37 in 10% MeOH in CH₂Cl₂) [20]. Fraction E4 (106.3 mg) was purified over semi-preparative HPLC in a gradient system [H₂O (A), CH₃CN (B); 0 min: 5% B > 0–17 min: 85.5% B > 17–20 min: 100% B, UV at 330 nm, 9.8 min], affording compound **2** (14.5 mg).

The *n*-hexane fraction (1.4 g) was chromatographed over a silica gel column and eluted with a stepwise gradient of *n*-hexane, ethyl acetate, and methanol to give six fractions (H1-H6). Fraction H1 (197.4 mg) was further chromatographed over a Sephadex-LH 20 column (100% CH₂Cl₂) to afford four subfractions (A-D). Purification of subfraction C

(29.1 mg) by silica gel CC (*n*-hex:CH₂Cl₂ 7:3) yielded peperobtusin A (5, 8.1 mg, $R_f = 0.76$ in 5% CH₃OH in CH₂Cl₂) [10]. Fraction H2 (279.6 mg) was chromatographed over a Sephadex LH-20 column (CH₂Cl₂:MeOH 1:1) to give five subfractions (A–E). Subfraction C (14.7 mg) was purified by silica gel CC (*n*-hex: CH₂Cl₂ 3:7–0:1) to afford peperomin B (6, 3.1 mg, $R_f = 0.04$ in CH₂Cl₂) [22].

The aqueous fraction (2.3 g) was fractionated over a Diaion-HP20 column eluted with an increasing solvent ratio of water and methanol to give five fractions (A1–A5). Fraction A3 (404.7 mg) was chromatographed over a Sephadex-LH20 column (100% MeOH) to afford seven subfractions (A–G). Subfraction B (55.2 mg) was further separated by silica gel CC (CH₂Cl₂:MeOH 7:3) to afford arabinothalictoside (7, 14.6 mg, $R_f = 0.57$ in 30% MeOH in CH₂Cl₂) [23]. Subfraction D (69.4 mg) was further chromatographed over a silica gel column (CH₂Cl₂:MeOH 8:2–0:1), yielding compound 1 (7.4 mg, $R_f = 0.88$ in 30% MeOH in CH₂Cl₂).

Peperomic ester (trimethyl (1*S*,2*R*)-1-(((*E*)-3-(3,4-dihydroxyphenyl)acryloyl)oxy)- propane-1,2,3-tricarboxylate, 1): brownish liquid; IR (ATR) ν_{\max} : 3402, 1715 cm⁻¹. UV λ_{\max} (MeOH) (log *e*) 218 (4.15), 333 nm (4.21); ¹H-NMR (400 MHz, CD₃OD): Table 1; ¹³C-NMR (100 MHz, CD₃OD): Table 1; negative-ion HR-ESI-MS *m/z* 395.0975 [M – H]⁻ (calcd. for C₁₈H₁₉O₁₀: 395.0984).

Peperoside (*N*-[2-(3,4-dihydroxyphenyl)ethyl]-3,4-dihydroxybenzamide 4'-*O*-β-D-glucoside, 2): white amorphous powder, IR (ATR) ν_{\max} : 3250, 2931, 2360, and 1607 cm⁻¹. UV λ_{\max} (log *e*) (MeOH) 290 (3.14), 317 nm (3.32). ¹H-NMR (400 MHz, CD₃OD): Table 2; ¹³C-NMR (100 MHz, CD₃OD): Table 2; negative-ion HR-ESI-MS *m/z* 450.1379 [M – H]⁻ (calcd. for C₂₁H₂₄NO₁₀: 450.1406).

3.4. Biological activities

3.4.1. Anthelmintic Activity

The anthelmintic bioassay was conducted by applying the method developed by Thomsen et al. using the model organism *C. elegans*, which was previously demonstrated to correlate with anthelmintic activity against parasitic trematodes [33]. The *C. elegans* Bristol N2 wild-type strain was obtained from the Caenorhabditis Genetic Center (CGC), Minnesota University, Minneapolis, USA. The nematodes were grown on petri plates of NGM (Nematode Growth Media) using uracil auxotroph *E. coli* strain OP50 as the food source. The solvent DMSO (2%) and the anthelmintic drug ivermectin (10 µg/mL, nearly 100% dead worms after 30 min incubation) were used as negative and positive controls in all assays, respectively. All assays were carried out in triplicate.

3.4.2. Antifungal Activity

The antifungal activity was examined against the phytopathogenic ascomycetes *B. cinerea* Pars and *S. tritici* Desm. and the oomycete *P. infestans* (Mont.) de Bary in 96-well microtiter plate assays according to protocols from the Fungicide Resistance Action Committee (FRAC) with minor modifications as described by Otto et al. [34]. Briefly, the isolated compounds were tested at the highest concentration of 125 µM, while the solvent DMSO was used as a negative control (max. concentration 2.5%). The commercially used fungicides, epoxiconazole and terbinafine (Sigma-Aldrich, Darmstadt, Germany), served as reference compounds. The pathogen growth was evaluated seven days after inoculation by measurement of the optical density (OD) at λ 405 nm with a TecanGENios Pro microplate reader (five measurements per well using multiple reads in 3 × 3 square). Each experiment was carried out in triplicate.

3.4.3. Antibacterial Activity

The isolated compounds (1 and 100 µM) were evaluated against the Gram-negative *A. fischerii* (DSM507) and the Gram-positive *B. subtilis* 168 (DSM 10), as described by dos Santos et al. [35]. The tests were conducted in 96-well plates based on the bioluminescence (*A. fisheri*) or absorption (*B. subtilis*) read-out. Chloramphenicol (100 µM) was

used as a positive control to induce complete inhibition of bacterial growth. The results (mean \pm standard deviation value, $n = 6$) are given in relation to the negative control (bacterial growth, 1% DMSO without test compound) as relative values (percent inhibition). Negative values indicate an increase in bacterial growth.

3.4.4. Cytotoxic Activity

The cytotoxicity and impact on the metabolic cell viability of isolated compounds at 10 nM and 10 μ M was evaluated against PC-3 (human prostate adenocarcinoma) and HT-29 (human colorectal adenocarcinoma) cancer cell lines. Both cell lines were purchased from ATCC (Manassas, VA, USA). The cell culture medium RPMI 1640, the supplements FCS and L-glutamine, as well as PBS and trypsin/EDTA were purchased from Capricorn Scientific GmbH (Ebsdorfergrund, Germany). Culture flasks, multi-well plates, and further cell culture plastics were from Greiner Bio-One GmbH (Frickenhausen, Germany) and TPP (Trasadingen, Switzerland), respectively. Resazurin used for the cell viability assays was purchased from Sigma-Aldrich GmbH (Taufkirchen, Germany). PC-3 and HT-29 cells were cultured in RPMI 1640 media supplemented with 10% heat-inactivated FCS, 2 mM L-glutamine, and 1% penicillin/streptomycin in a humidified atmosphere with 5% CO₂ at 37 °C. Routinely, cells were cultured in T-75 flasks until reaching subconfluency (~80%); subsequently, cells were harvested by washing with PBS and detaching by using trypsin/EDTA (0.05% in PBS) prior to cell passaging and seeding for subculturing and assays in 96-well plates, respectively [36].

The cell handling and assay techniques were in accordance with the method described by Khan et al. [36]. In brief, antiproliferative and cytotoxic effects of the compounds were investigated by performing colorimetric MTT (3-(4,5-dimethylthiazol-2-yl)-2,5-diphenyltetrazolium bromide) and CV (crystal violet)-based cell viability assays (Sigma-Aldrich, Taufkirchen, Germany), respectively. For this purpose, cells were seeded in low densities in 96-well plates using the aforementioned cell culture medium. The cells were allowed to adhere for 24 h, followed by the 48 h compound treatment. Based on 20 mM DMSO stock solutions, the compounds were serially diluted in standard growth media to reach final concentrations of 100, 50, 25, 12.5, 6.25, 3.125, and 1.56 μ M for cell treatment. For control measures, cells were treated in parallel with 125 μ M digitonin (positive control, for data normalization set to 0% cell viability). Each data point was determined in technical quadruplicates and two independent biological replicates. As soon as the 48 h incubation was finished, cell viability was measured.

For the MTT assay, cells were washed once with PBS, followed by incubation with MTT working solution (0.5 mg/mL MTT in culture medium) for 1 h under standard growth conditions. After discarding the MTT solution, DMSO was added in order to dissolve the formed formazan, followed by measuring formazan absorbance at 570 nm, and additionally, at the reference/background wavelength of 670 nm by using a SpectraMax M5 multi-well plate reader (Molecular Devices, San Jose, CA, USA).

For the CV assay, cells were washed once with PBS and fixed with 4% paraformaldehyde (PFA) for 20 min at room temperature (RT). After discarding the PFA solution, the cells were left to dry for 10 min and then stained with 1% crystal violet solution for 15 min at RT. The cells were washed with water and dried overnight at RT. Afterwards, acetic acid (33% in ultrapure water) was added to the stained cells and absorbance was measured at 570 nm and 670 nm (reference wavelength) using a SpectraMax M5 multi-well plate reader (Molecular Devices, San Jose, CA, USA). For data analyses, GraphPad Prism version 8.0.2, SigmaPlot 14.0 and Microsoft Excel 2013 were used.

The results are shown as a percentage of the control values obtained from untreated cultures, i.e. cell viability in percent.

4. Conclusions

The present investigation of a methanol extract from the leaves of *P. obtusifolia* led to the isolation of two new compounds named peperomic ester (1) and peperoside (2), along with

five known compounds. The isolated compounds were evaluated for their anthelmintic, antifungal, antibacterial, and anticancer activities. Peperoside (2) and its related compounds (3, 4) have the advantage of low activity against all organisms/cells tested. Since similar phenethylamides show taste and neuroactive properties [37,38]—which were not part of this study—their use in such tests, which usually include human panels or animals, appears acceptable.

The known peperobtusin A (5) was the most active compound against *B. subtilis* and showed an antiproliferative and cytotoxic effect in the lower micromolar concentration range towards human PC-3 (prostate) and HT-29 (colon) cancer cell lines. The observed antibacterial activity supports the traditional use of *P. obtusifolia* as a skin cleanser. These findings suggest that *P. obtusifolia* might have some general toxicity and thus should be used with care in applications where cytotoxicity is not desired. However, prenylated benzopyran derivatives structurally related to 5 were shown to exhibit selective activity against breast cancer cells but did not influence normal breast cells [39]. The impact of this compound class on the mitochondrial respiratory chain [39,40] and their function as PPAR agonists may play a role in compound selectivity [41]. Thus, more extensive and detailed studies on the anticancer activity of natural prenylated benzopyrans should be undertaken in order to provide an understanding of structural requirements (SAR) for such cytotoxic (or other) activity.

Supplementary Materials: The following supporting information can be downloaded at: <https://www.mdpi.com/article/10.3390/molecules27144363/s1>, Figure S1: ^1H NMR spectrum of compound 1 (400 MHz, $\text{MeOH-}d_4$), Figure S2: ^{13}C NMR spectrum of compound 1 (100 MHz, $\text{MeOH-}d_4$), Figure S3: HSQC spectrum of compound 1 (400 MHz, $\text{MeOH-}d_4$), Figure S4: HMBC spectrum of compound 1 (400 MHz, $\text{MeOH-}d_4$), Figure S5: $^1\text{H-}^1\text{H}$ COSY spectrum of compound 1 (400 MHz, $\text{MeOH-}d_4$), Figure S6: UV spectrum of compound 1 in MeOH, Figure S7: IR spectrum of compound 1 in MeOH, Figure S8: ESI-HRMS spectrum of compound 1 in negative ion mode, Figure S9: HRMS spectrum from ethanol extract of *P. obtusifolia* with selected molecular ion of m/z 395.0979 $[\text{M} - \text{H}]^-$, Figure S10: ^1H NMR spectrum of compound 2 (400 MHz, $\text{MeOH-}d_4$), Figure S11: ^{13}C NMR spectrum of compound 2 (100 MHz, $\text{MeOH-}d_4$), Figure S12: DEPT135 spectrum of compound 2 (100 MHz, $\text{MeOH-}d_4$), Figure S13: HSQC spectrum of compound 2 (400 MHz, $\text{MeOH-}d_4$), Figure S14: HMBC spectrum of compound 2 (400 MHz, $\text{MeOH-}d_4$), Figure S15: $^1\text{H-}^1\text{H}$ COSY spectrum of compound 2 (400 MHz, $\text{MeOH-}d_4$), Figure S16: 1D-ROESY spectrum of compound 2 (400 MHz, $\text{MeOH-}d_4$), Figure S17: UV spectrum of compound 2 in MeOH, Figure S18: IR spectrum of compound 2 in MeOH, Figure S19: ESI-HRMS spectrum of compound 2 in negative ion mode, Figure S20. Isolation scheme for compounds 1–7, Table S1: Polarimeter data of compound 1.

Author Contributions: Conceptualization, L.A.W.; methodology, I.W. and K.F.; formal analysis, I.W., K.F., H.H., I.M. and R.R.; investigation, I.W.; resources, L.A.W.; data curation, I.W. and K.F.; writing—original draft preparation, I.W., K.F. and R.R.; writing—review and editing, I.W., R.R., K.F. and L.A.W.; supervision, K.F. and L.A.W.; project administration, K.F. and L.A.W.; funding acquisition, I.W. and L.A.W. All authors have read and agreed to the published version of the manuscript.

Funding: This study was supported by the German Academic Exchange Service (DAAD) as a grant scholarship part of the Ph.D. thesis of I.W. Funding program/-ID: Research Grants—Doctoral Programs in Germany, 2017/18 (57299294), ST34. The funder had no role in the study design, decision to publish, or manuscript preparation.

Institutional Review Board Statement: Not applicable.

Informed Consent Statement: Not applicable.

Data Availability Statement: The data presented in this study are available on request from the corresponding author.

Acknowledgments: The authors are indebted to Anke Dettmer, Mthandazo Dube, and Martina Lerbs (all IPB Halle) for their performance of antibacterial, antifungal, anthelmintic, and anticancer bioassays, respectively. Thanks to Andrea Porzel and Gudrun Hahn (IPB Halle) for NMR measurements and Mandy Dorn for HRMS measurements.

Conflicts of Interest: The authors declare that they have no known competing financial interest or personal relationships that could have appeared to influence the work reported in this paper.

References

1. Felipe, L.G.; Baldoqui, D.C.; Kato, M.J.; Bolzani, V.d.S.; Guimarães, E.F.; Cicarelli, R.M.B.; Furlan, M. Trypanocidal tetrahydrofuran lignans from *Peperomia blanda*. *Phytochemistry* **2008**, *69*, 445–450. [[CrossRef](#)] [[PubMed](#)]
2. Al-Madhagi, W.M.; Mohd Hashim, N.; Awad Ali, N.A.; Alhadi, A.A.; Abdul Halim, S.N.; Othman, R. Chemical profiling and biological activity of *Peperomia blanda* (Jacq.) Kunth. *PeerJ* **2018**, *6*, e4839. [[CrossRef](#)] [[PubMed](#)]
3. Malquichagua Salazar, K.J.; Delgado Paredes, G.E.; Lluncor, L.R.; Young, M.C.M.; Kato, M.J. Chromenes of polyketide origin from *Peperomia villipetiola*. *Phytochemistry* **2005**, *66*, 573–579. [[CrossRef](#)] [[PubMed](#)]
4. Seeram, N.P.; Lewis, A.W.; Jacobs, H.; Nair, M.G.; McLean, S.; Reynolds, W.F. Proctoriones A–C: 2-Acylcyclohexane-1,3-dione derivatives from *Peperomia proctorii*. *J. Nat. Prod.* **2000**, *63*, 399–402. [[CrossRef](#)] [[PubMed](#)]
5. Wu, J.; Li, N.; Hasegawa, T.; Sakai, J.; Kakuta, S.; Tang, W.; Oka, S.; Kiuchi, M.; Ogura, H.; Kataoka, T.; et al. Bioactive tetrahydrofuran lignans from *Peperomia dindygulensis*. *J. Nat. Prod.* **2005**, *68*, 1656–1660. [[CrossRef](#)] [[PubMed](#)]
6. Xu, S.; Li, N.; Ning, M.M.; Zhou, C.H.; Yang, Q.R.; Wang, M.W. Bioactive compounds from *Peperomia pellucida*. *J. Nat. Prod.* **2006**, *69*, 247–250. [[CrossRef](#)] [[PubMed](#)]
7. Li, N.; Wu, J.; Hasegawa, T.; Sakai, J.; Bai, L.; Wang, L.; Kakuta, S.; Furuya, Y.; Ogura, H.; Kataoka, T.; et al. Bioactive polyketides from *Peperomia duclouxii*. *J. Nat. Prod.* **2007**, *70*, 998–1001. [[CrossRef](#)] [[PubMed](#)]
8. Wang, X.; Cheng, Y.; Wu, H.; Li, N.; Liu, R.; Yang, X.; Qiu, Y.Y.; Wen, H.; Liang, J. The natural secolignan peperomin E induces apoptosis of human gastric carcinoma cells via the mitochondrial and PI3K/Akt signaling pathways in vitro and in vivo. *Phytomedicine* **2016**, *23*, 818–827. [[CrossRef](#)] [[PubMed](#)]
9. Batista, A.N.L.; Santos-Pinto, J.; Batista, J.M., Jr.; Souza-Moreira, T.M.; Santoni, M.M.; Zanelli, C.F.; Kato, M.J.; López, S.N.; Palma, M.S.; Furlan, M. The combined use of proteomics and transcriptomics reveals a complex secondary metabolite network in *Peperomia obtusifolia*. *J. Nat. Prod.* **2017**, *80*, 1275–1286. [[CrossRef](#)]
10. Tanaka, T.; Asai, F.; Iinuma, M. Phenolic compounds from *Peperomia obtusifolia*. *Phytochemistry* **1998**, *49*, 229–232. [[CrossRef](#)]
11. da Silva Mota, J.; Leite, A.C.; Batista Junior, J.M.; Noeli López, S.; Luz Ambrósio, D.; Duó Passerini, G.; Kato, M.J.; da Silva Bolzani, V.; Barretto Cicarelli, R.M.; Furlan, M. In vitro trypanocidal activity of phenolic derivatives from *Peperomia obtusifolia*. *Planta Med.* **2009**, *75*, 620–623. [[CrossRef](#)]
12. Mota, J.d.S.; Leite, A.C.; Kato, M.J.; Young, M.C.M.; Bolzani, V.d.S.; Furlan, M. Isoswertisin flavones and other constituents from *Peperomia obtusifolia*. *Nat. Prod. Res.* **2011**, *25*, 1–7. [[CrossRef](#)] [[PubMed](#)]
13. Batista, J.M.; Batista, A.N.L.; Kato, M.J.; Bolzani, V.S.; López, S.N.; Nafie, L.A.; Furlan, M. Further monoterpene chromane esters from *Peperomia obtusifolia*: VCD determination of the absolute configuration of a new diastereomeric mixture. *Tetrahedron Lett.* **2012**, *53*, 6051–6054. [[CrossRef](#)]
14. Ruiz Mostacero, N.; Castelli, M.V.; Cutró, A.C.; Hollmann, A.; Batista, J.M., Jr.; Furlan, M.; Valles, J.; Fulgueira, C.L.; López, S.N. Antibacterial activity of prenylated benzopyrans from *Peperomia obtusifolia* (Piperaceae). *Nat. Prod. Res.* **2021**, *35*, 1706–1710. [[CrossRef](#)] [[PubMed](#)]
15. Tamayose, C.I.; Romoff, P.; Toyama, D.O.; Gaeta, H.H.; Costa, C.R.C.; Belchor, M.N.; Ortolan, B.D.; Velozo, L.S.M.; Kaplan, M.A.C.; Ferreira, M.J.P.; et al. Non-clinical studies for evaluation of 8-c-rhamnosyl apigenin purified from *Peperomia obtusifolia* against acute edema. *Int. J. Mol. Sci.* **2017**, *18*, 1972. [[CrossRef](#)]
16. Wu, W.; Zhao, F.; Ding, R.; Bao, L.; Gao, H.; Lu, J.C.; Yao, X.S.; Zhang, X.Q.; Liu, H.W. Four new cryptoporin acid derivatives from the fruiting bodies of *Cryptoporus sinensis*, and their inhibitory effects on nitric oxide production. *Chem. Biodivers.* **2011**, *8*, 1529–1538. [[CrossRef](#)]
17. Zhou, L.Y.; Yu, X.H.; Lu, B.; Hua, Y. Bioassay-guided isolation of cytotoxic isocryptoporin acids from *Cryptoporus volvatus*. *Molecules* **2016**, *21*, 1692. [[CrossRef](#)] [[PubMed](#)]
18. Pham, H.T.; Lee, K.H.; Jeong, E.; Woo, S.; Yu, J.; Kim, W.Y.; Lim, Y.W.; Kim, K.H.; Kang, K.B. Species prioritization based on spectral dissimilarity: A case study of polyporoid fungal species. *J. Nat. Prod.* **2021**, *84*, 298–309. [[CrossRef](#)] [[PubMed](#)]
19. Chepkirui, C.; Yuyama, K.T.; Wanga, L.A.; Decock, C.; Matasyoh, J.C.; Abraham, W.-R.; Stadler, M. Microporenic acids A–G, biofilm inhibitors, and antimicrobial agents from the Basidiomycete *Microporus* species. *J. Nat. Prod.* **2018**, *81*, 778–784. [[CrossRef](#)]
20. Liao, Y.; Ye, Y.; Li, S.; Zhuang, Y.; Chen, L.; Chen, J.; Cui, Z.; Huo, L.; Liu, S.; Song, G. Synthesis and SARs of dopamine derivatives as potential inhibitors of influenza virus PAN endonuclease. *Eur. J. Med. Chem.* **2020**, *189*, 112048. [[CrossRef](#)]
21. Park, J.B. Protective effects of veskamide, enferamide, becatamide, and oretamide on H₂O₂-induced apoptosis of PC-12 cells. *Phytomedicine* **2011**, *18*, 843–847. [[CrossRef](#)] [[PubMed](#)]
22. Chen, C.-M.; Jan, F.Y.; Chen, M.-T.; Lee, T.-J. Peperomins A, B, and C, novel secolignans from *Peperomia japonica*. *Heterocycles* **1989**, *29*, 411–414. [[CrossRef](#)]
23. Li, H.X.; Yang, S.Y.; Kim, Y.S.; Jang, H.D.; Kim, Y.H.; Li, W. Nitro derivatives and other compounds from sugar apple (*Annona squamosa* L.) leaves exhibit soluble epoxide hydrolase inhibitory activity. *Med. Chem. Res.* **2019**, *28*, 1939–1944. [[CrossRef](#)]
24. Li, Y.Z.; Tong, A.P.; Huang, J. Two new norlignans and a new lignanamide from *Peperomia tetraphylla*. *Chem. Biodivers.* **2012**, *9*, 769–776. [[CrossRef](#)]

25. Yoshikawa, M.; Yamaguchi, S.; Murakami, T.; Matsuda, H.; Yamahara, J.; Murakami, N. Absolute stereostructures of trifoliones A, B, C, and D, new biologically active diterpenes from the tuber of *Sagittaria trifolia* L. *Chem. Pharm. Bull.* **1993**, *41*, 1677–1679. [[CrossRef](#)] [[PubMed](#)]
26. Zhou, Z.; Luo, J.; Pan, K.; Kong, L. A new alkaloid glycoside from the rhizomes of *Aristolochia fordiana*. *Nat. Prod. Res.* **2014**, *28*, 1065–1069. [[CrossRef](#)]
27. Alves, N.S.F.; Setzer, W.N.; da Silva, J.K.R. The chemistry and biological activities of *Peperomia pellucida* (Piperaceae): A critical review. *J. Ethnopharmacol.* **2019**, *232*, 90–102. [[CrossRef](#)]
28. Ng, Z.X.; Than, M.J.Y.; Yong, P.H. *Peperomia pellucida* (L.) Kunth herbal tea: Effect of fermentation and drying methods on the consumer acceptance, antioxidant and anti-inflammatory activities. *Food Chem.* **2021**, *344*, 128738. [[CrossRef](#)]
29. Gutierrez, Y.V.; Yamaguchi, L.F.; de Moraes, M.M.; Jeffrey, C.S.; Kato, M.J. Natural products from *Peperomia*: Occurrence, biogenesis and bioactivity. *Phytochem Rev.* **2016**, *15*, 1009–1033. [[CrossRef](#)]
30. Batista, J.M., Jr.; Lopez, S.N.; Mota Jda, S.; Vanzolini, K.L.; Cass, Q.B.; Rinaldo, D.; Vilegas, W.; Bolzani Vda, S.; Kato, M.J.; Furlan, M. Resolution and absolute configuration assignment of a natural racemic chromane from *Peperomia obtusifolia* (Piperaceae). *Chirality* **2009**, *21*, 799–801. [[CrossRef](#)]
31. Shi, L.; Qin, H.; Jin, X.; Yang, X.; Lu, X.; Wang, H.; Wang, R.; Yu, D.; Feng, B. The natural phenolic peperobtusin A induces apoptosis of lymphoma U937 cells via the Caspase dependent and p38 MAPK signaling pathways. *Biomed. Pharmacother.* **2018**, *102*, 772–781. [[CrossRef](#)] [[PubMed](#)]
32. Seeram, N.P.; Jacobs, H.; McLean, S.; Reynolds, W.F. A prenylated benzopyran derivative from *Peperomia clusiifolia*. *Phytochemistry* **1998**, *49*, 1389–1391. [[CrossRef](#)]
33. Thomsen, H.; Reider, K.; Franke, K.; Wessjohann, L.A.; Keiser, J.; Dagne, E.; Arnold, N. Characterization of constituents and anthelmintic properties of *Hagenia abyssinica*. *Sci. Pharm.* **2012**, *80*, 433–446. [[CrossRef](#)] [[PubMed](#)]
34. Otto, A.; Porzel, A.; Schmidt, J.; Brandt, W.; Wessjohann, L.; Arnold, N. Structure and absolute configuration of pseudohygrophorones A¹² and B¹², alkyl cyclohexenone derivatives from *Hygrophorus abieticola* (Basidiomycetes). *J. Nat. Prod.* **2016**, *79*, 74–80. [[CrossRef](#)] [[PubMed](#)]
35. dos Santos, C.H.C.; de Carvalho, M.G.; Franke, K.; Wessjohann, L. Dammarane-type triterpenoids from the stem of *Ziziphus glaziovii* Warm. (Rhamnaceae). *Phytochemistry* **2019**, *162*, 250–259. [[CrossRef](#)] [[PubMed](#)]
36. Khan, M.F.; Nasr, F.A.; Noman, O.M.; Alyhya, N.A.; Ali, I.; Saoud, M.; Rennert, R.; Dube, M.; Hussain, W.; Green, I.R.; et al. Cichorins D-F: Three new compounds from *Cichorium intybus* and their biological effects. *Molecules* **2020**, *25*, 4160. [[CrossRef](#)]
37. Krammer, G.; Ley, J.P.; Geißler, K.; Geißler, T.; Gomoll, F.; Welters, P.; Jach, G.; Wessjohann, L. Method for Biotechnological Production of Methylized Cinnamic Acids and Cinnamic Acid Esters, Methylized Phenethylamines and the Coupling Products Thereof, Particularly of Cinnamic Acid Amides. U.S. Patent US10227620B2, 12 March 2019.
38. Greger, H. Alkamides: A critical reconsideration of a multifunctional class of unsaturated fatty acid amides. *Phytochem. Rev.* **2016**, *15*, 729–770. [[CrossRef](#)]
39. Taha, H.; Looi, C.Y.; Arya, A.; Wong, W.F.; Yap, L.F.; Hasanpourghadi, M.; Mohd, M.A.; Paterson, I.C.; Ali, H.A. (6E,10E) Isopolycerasoidol and (6E,10E) isopolycerasoidol methyl ester, prenylated benzopyran derivatives from *Pseuduvaria monticola* induce mitochondrial-mediated apoptosis in human breast adenocarcinoma cells. *PLoS ONE* **2015**, *10*, e0126126. [[CrossRef](#)] [[PubMed](#)]
40. Zafra-Polo, M.C.; González, M.C.; Tormo, J.R.; Estornell, E.; Cortes, D. Polyalthidin: New prenylated benzopyran inhibitor of the mammalian mitochondrial respiratory chain. *J. Nat. Prod.* **1996**, *10*, 913–916. [[CrossRef](#)] [[PubMed](#)]
41. Corés Martínez, D.M.; Sanz Ferrando, M.J.; Bermejo del Castillo, A.; Piqueras Ruiz, L.; Collado Sánchez, A.; Gomes Marques, P.; Vila Dasí, L. Prenylated Benzopyranes as PPAR. Agonists Patent WO2019129909, 4 July 2019.